ACS OMEGA

http://pubs.acs.org/journal/acsodf

Article

Anion Exchange Membranes Based on Bis-Imidazolium and Imidazolium-Functionalized Poly(phenylene oxide) for Vanadium Redox Flow Battery Applications

Jing Li, Fei Xu, Weishu Chen, Yuyang Han, and Bencai Lin*

Cite This: *ACS Omega* 2023, 8, 16506−16512

Read Online

ACCESS | Metrics & More | Article Recommendations | Supporting Information

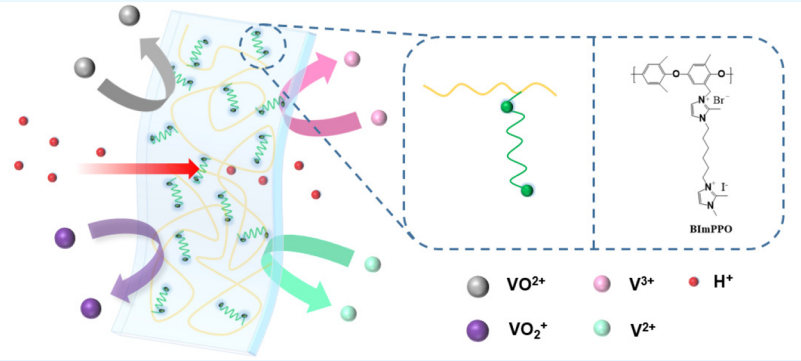

ABSTRACT: Although the Nafion membrane has a high energy efficiency, long service life, and operational flexibility when applied for vanadium redox flow battery (VRFB) applications, its applications are limited due to its high vanadium permeability. In this study, anion exchange membranes (AEMs) based on poly(phenylene oxide) (PPO) with imidazolium and bis-imidazolium cations were prepared and used in VRFBs. PPO with long-pendant alkyl-side-chain bis-imidazolium cations (BImPPO) exhibits higher conductivity than the imidazolium-functionalized PPO with short chains (ImPPO). ImPPO and BImPPO have a lower vanadium permeability (3.2×10^{-9} and 2.9×10^{-9} cm^2 s^{-1}) than Nafion 212 (8.8×10^{-9} cm^2 s^{-1}) because the imidazolium cations are susceptible to the Donnan effect. Furthermore, under the current density of 140 mA cm^{-2}, the VRFBs assembled with ImPPO- and BImPPO-based AEMs exhibited a Coulombic efficiency of 98.5% and 99.8%, respectively, both of which were higher than that of the Nafion212 membrane (95.8%). Bis-imidazolium cations with long-pendant alkyl side chains contribute to hydrophilic/hydrophobic phase separation in the membranes, thus improving the conductivity of membranes and the performance of VRFBs. The VRFB assembled with BImPPO exhibited a higher voltage efficiency (83.5%) at 140 mA cm^{-2} than that of ImPPO (77.2%). These results of the present study suggest that the BImPPO membranes are suitable for VRFB applications.

1. INTRODUCTION

Vanadium redox flow batteries (VRFBs) have attracted great attention for their long service life, operational flexibility, and environmental friendliness.[1−3] An important component of VRFBs, the ion-exchange membrane (IEM), is used to separate the anode of VRFBs from their cathode.[4,5] The low vanadium permeability, high conductivity, and robust chemical stability are required for an ideal IEM in the application of VRFBs.[6] Currently, Nafion membranes are commonly used as IEMs in VRFBs owing to their high conductivity.[7−9] However, the high vanadium permeability of Nafion significantly hinders its commercialization in this field.[5,7] Recently, sulfonated poly(arylene ether) has been widely used as an IEM material for VRFBs because of its high conductivity and good chemical stability.[10,11] Nevertheless, the high vanadium permeability of sulfonated poly(arylene ether) membranes remains unresolved.[12−14]

More recently, the usage of AEMs in VRFB applications has attracted great attention because of the low vanadium permeability resulting from the effects of Donnan exclusion on the AEMs cations.[15,16] AEMs containing quaternary ammonium,[15,16] imidazolium,[17] and pyridinium[18] cations have been investigated for VRFB applications, and those with imidazolium cations have exhibited good performance.[19−22]

The ion-exchange capacity (IEC) and ionic cluster distribution in the membrane are known to influence the

Received: March 19, 2023
Accepted: April 18, 2023
Published: April 27, 2023

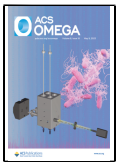

Scheme 1. Preparation of Bis-Imidazolium Salt

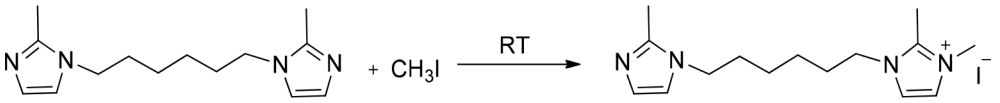

Scheme 2. Preparation of ImPPO and BImPPO Membrane

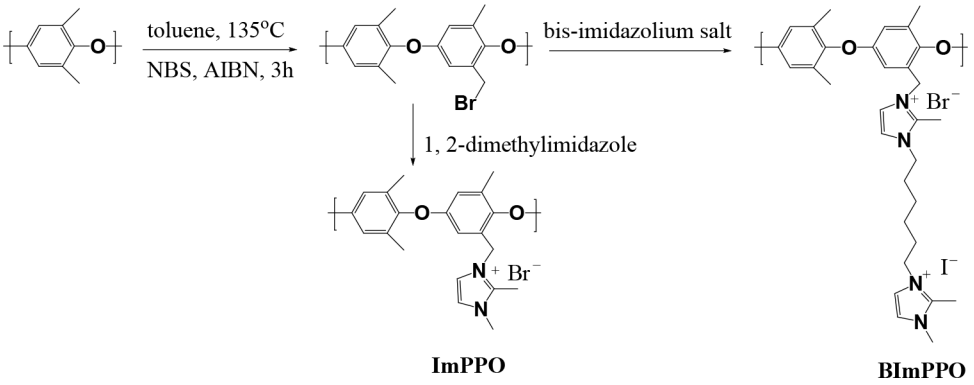

conductivity of the membranes.[23,24] Generally, high IEC value resulted in the high conductivity of the AEMs, while it also led to mechanical degradation of the membranes. Recent research indicated that AEMs with hydrophilic/hydrophobic microphase separation possess high conductivity owing to the formation of an ion transport channel.[25−31] In addition, the hydrophobic phase of the membranes could decrease their dimensional swelling and maintain the mechanical properties. Strategies like the synthesis of quaternized block,[32] cluster,[33] comb-shaped,[34] and grafted polymers have been used to fabricate microphase separation structures to improve the conductivity of AEMs.

Inspired by the chemical structure of Nafion, poly(phenylene oxide) (PPO) functionalized with long-pendant alkyl-side-chain bis-imidazolium cations (BImPPO) was designed and synthesized. For comparison, imidazolium-functionalized PPO without a long-pendant alkyl side chain (ImPPO) was synthesized and investigated under the same conditions. The introduction of long-pendant bis-imidazolium cations to PPO is expected to lead to hydrophilic/hydrophobic microphase separation in the membranes, resulting in an increase in conductivity.

The properties of the ImPPO, BImPPO, and Nafion212 membranes, including their chemical structure, swelling ratio (SR), area resistance (AR), water uptake (WU), chemical stability, microphase morphology, mechanical performance, vanadium permeability, conductivity, and VRFB performance were comprehensively studied.

2. EXPERIMENTAL SECTION

2.1. Materials. PPO, 1,6-dibromohexane, *N*-methylimidazole, iodomethane, 2-methylimidazole, azodiisobutyronitrile (AIBN), acetonitrile, chlorobenzene, *N*-methyl pyrrolidone (NMP), ethyl acetate, anhydrous ether, N-bromosuccinimide (NBS), anhydrous ethanol, sulfuric acid (H_2SO_4, 98%), and dichloromethane were used as purchased.

2.2. Synthesis of Brominated Poly(phenylene oxide) (BPPO) and Bis-Imidazolium Salt. BPPO with a certain degree of bromination (DB) and 2,3-dimethyl-1-(6-(2-methylimidazol-1-yl)hexyl)-imidazolium iodide (bis-imidazolium salt) were synthesized as documented in our previous work (Scheme 1).[31]

2.3. Preparation of the Imidazolium Functionazized PPO (ImPPO) and Bis-Imidazolium Functionalized (BImPPO) Membranes. Im-PPO and BIm-PPO were obtained as follows: a 5 wt % polymer solution was obtained by dissolving BrPPO in NMP, then 1,2-dimethylimidazole or bis-imidazolium salt (molar ratio is 1:1) was added into the solution. The mixture solution was stirred for 24 h at 50 °C for 24 h, and the produced polymers were precipitated by methylbenzene and noted as Im-PPO and BIm-PPO, respectively (Scheme 2). The PPO and BImPPO membranes were obtained by casting an NMP solution of Im-PPO or BIm-PPO onto a Teflon template. The Teflon template was dried for 48 and 24 h at 70 and 80 °C, respectively. All of the produced membranes with a thickness of ∼50 μm were immersed in 1 M H_2SO_4 for 24 h before characterization. The characterization of polymers and membranes is described in the Supporting Information.

2.4. Characterization. ^{1}H NMR spectra of ImPPO, BImPPO, BrPPO and 2,3-dimethyl-1-(6-(2-methylimidazol-1-yl)hexyl)-imidazolium iodide were recorded on a Varian 400 MHz spectrometer (Varian CP-3800). The mechanical properties of ImPPO- and BImPPO-based membranes were studied using an Instron 3365 at 25 °C. The microstructure of ImPPO and BImPPO-based membranes was investigated using an atom force microscope (AFM). The conductivity of ImPPO- and BImPPO-based membranes was measured on an electrochemical workstation (CHI660E). The water uptake (WU), conductivity, swelling ratio (SR), and ion exchange capacity (IEC) of ImPPO and BImPPO membranes were measured as described in a previous paper.[21]

2.5. Chemical Stability. The chemical stability of the ImPPO- and BImPPO-based membranes was tested in a solution that contained VO^{2+} ions; a dry membrane with a known weight (W) was immersed in an electrolyte solution of 1.5 M VO^{2+}(VO_2^+)/3 M H_2SO_4 solution for 30 days at 25 °C. Then, the sample was taken out and rinsed with water. Another weight (W_0) was obtained after it was dried until its mass was no longer decreasing. The chemical stability of the ImPPO- and BImPPO-based membranes was evaluated by detecting the

https://doi.org/10.1021/acsomega.3c01846
ACS Omega 2023, 8, 16506−16512

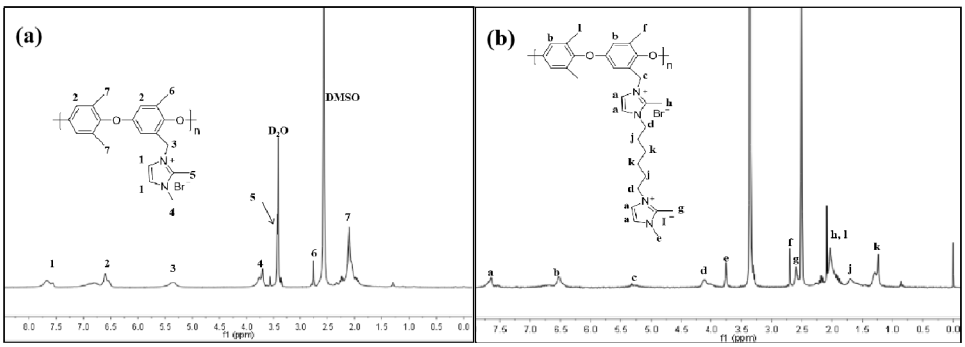

Figure 1. ^{1}H NMR of ImPPO (a) and BImPPO (b).

Table 1. IEC, WU, SR, Conductivity, and AR of Membranes

membrane samples	IEC (mmol/g)	WU (%)	SR (%)	conductivity (mS cm^{-1})	AR (Ω cm^2)
Nafion212	0.86 ± 0.1	19.9 ± 1.5	20.3 ± 1.0	45.2 ± 2.5	0.40 ± 0.1
ImPPO	2.28 ± 0.2	41.1 ± 2.0	36.7 ± 1.5	51.2 ± 3.0	0.23 ± 0.1
BImPPO	2.30 ± 0.3	45.5 ± 2.5	32.4 ± 1.0	60.4 ± 2.0	0.21 ± 0.1

changes on their weight, and it can be expressed by the following equation:

$$\text{Weight loss} = \frac{W - W_0}{W_0} \times 100\%$$

2.6. Vanadium Permeability. The vanadium permeability of membranes was measured as described in our previous work.[10]

2.7. Area Resistance. The IEMs were assembled in an conductive cell containing two compartments filled with 0.5 M sulfuric acid solution; the area resistance (AR) of the membrane was measured using an electrochemical workstation (CHI660 E). The ARs of ImPPO- and BImPPO-based membranes were obtained via the equation:

$$\text{AR} = (R_1 - R_2) \times S$$

where R_1 is the impedance of the conductive cell equipped with the obtained membranes, and R_2 is the impedance of the conductive cell without membranes. S is the effective area of the ImPPO- and BImPPO-based membranes.

2.8. Single-Cell Performance. The test system used in this single-cell test is the LANHE battery test system (CT 2001A-5 V/3A8CT-Q). The positive and negative electrolytes of the single cell are 1.5 M VO^{2+}(VO^{2+})/3.0 M H_2SO_4 solution and 1.5 M V^{2+}(V^{3+})/3.0 M H_2SO_4 solution, respectively. The electrodes and the collector plate both are made of graphite. The voltage for charging and discharging ranged from 0.7 to 1.6 V, and nitrogen was continuously purged to the negative electrolyte to ensure the stability of the battery. The Coulombic efficiency (CE), energy efficiency (EE), and voltage efficiency (VE) were calculated using the following equations:

$$\text{CE}\ (\%) = \frac{\text{discharge capacity (mAh)}}{\text{charge capacity (mAh)}} \times 100\%$$

$$\text{EE}\ (\%) = \frac{\text{discharge energy (mWh)}}{\text{charge energy (mWh)}} \times 100\%$$

$$\text{VE}\ (\%) = \frac{\text{EE}}{\text{CE}} \times 100\%$$

3. RESULTS AND DISCUSSION

3.1. Chemical Structures. In this study, PPO-based membranes with short- or long-pendant alkyl-side-chain imidazolium groups were prepared (Scheme 2). Figure S1 shows the chemical structure and ^{1}H NMR spectra of BrPPO and bis-imidazolium salt. The chemical shifts at 6.48−6.71 ppm were attributed to protons on the aromatic ring (Figure S1a). The signals at 2.10 and 2.80 ppm are attributable to the $-CH_3$ on the aromatic ring. The chemical shift of $-CH_2Br$ appears at 4.40 ppm. Figure S1b shows the expected chemical shifts of the bis-imidazolium salts. The ^{1}H NMR spectrum of ImPPO reveals chemical shifts at 7.46−7.49 ppm, which are attributable to the protons at the C4 and C5 positions of the imidazolium ring (Figure 1a). The chemical shift at 5.28 ppm represents the proton of $-CH_2-$. The peaks of the methyl group on the imidazolium ring can be found at 3.30 and 3.56−3.70 ppm, and the methyl group on the benzene rings can be found at 2.69 and 1.87−2.20 ppm, respectively. In the ^{1}H NMR spectrum of BImPPO, the signal at 7.70 ppm is associated with the protons at the C4 and C5 positions of the imidazolium ring, the chemical shifts at 5.32 ppm are attributable to the methylene that connects the imidazolium ring and benzene ring on the imidazolium ring, and the peak at 6.52 ppm is attributable to the protons on the benzene ring. The ^{1}H NMR spectrum of BImPPO has peaks at 4.12, 1.75, and 1.23 ppm that are not present in the ^{1}H NMR spectrum of ImPPO (Figure 1b). These peaks are attributable to the alkyl side chain. These results indicate the successful synthesis of BrPPO bis-imidazolium salts, ImPPO, and BImPPO.

3.2. Membrane Properties. Generally, the high IEC and WU of membranes favor the transportation of ions, which increases their conductivity. However, a high WU usually leads to reduced mechanical properties and an increase in the vanadium permeability of membranes. The IEC, WU, SR, conductivity, and AR of the ImPPO, BImPPO, and Nafion212 membranes are listed in Table 1. At 25 °C, the WU and SR for the ImPPO membrane were 41.1% and 45.5%, and those for the BImPPO membrane were 36.7% and 32.4%, respectively. All of these values are higher than those for Nafion212 (19.9% and 20.3%, respectively). The ImPPO and BImPPO membranes exhibited a higher WU and IEC than those of

https://doi.org/10.1021/acsomega.3c01846
ACS Omega 2023, 8, 16506−16512

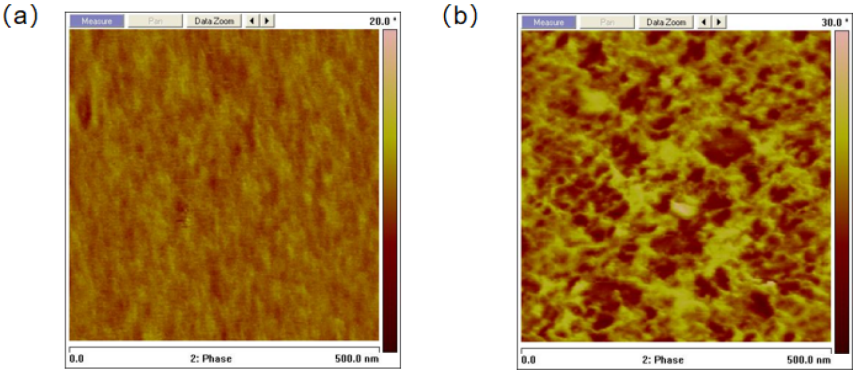

Figure 2. AFM phase images of ImPPO (a) and BImPPO membranes (b).

Nafion212. Therefore, unsurprisingly, the PPO-based AEMs had a lower AR (0.23 and 0.21 Ω cm^2) than Nafion212 (0.40 Ω cm^2). The AR of the IEM has a considerable influence on the voltage efficiency (VE) of VRFBs,[35] and the AR of the membranes increases with decreasing conductivity (Table 1). The ImPPO and BImPPO membranes exhibited conductivities of 51.2 and 60.4 mS cm^{-1}, respectively. Although the BImPPO and ImPPO membranes possess similar IECs, the BImPPO membrane had higher conductivity than that of the ImPPO membrane under the same conditions, probably due to the formation of hydrophilic/hydrophobic microphase separations resulting from the introduction of long-pendant bis-imidazolium cations, as supported by the AFM images (Figure 2).

The microphase morphologies of the ImPPO and BImPPO membranes were studied using AFM (Figure 2). The dark region in the phase images consists of hydrophilic imidazolium groups, and the hydrophobic PPO backbones appear as bright regions.[31] Compared with the ImPPO membrane, the BImPPO membrane exhibited marked hydrophilic/hydrophobic microphase separation, owing to the presence of the long-pendant alkyl-side-chain bis-imidazolium cations. The hydrophilic/hydrophobic microphase separation facilitated ion transportation in the membranes, thus improving their conductivity.

3.3. Mechanical Property and Chemical Stability. Both the mechanical property and chemical stability of membranes are important for VRFB applications. The BImPPO and ImPPO membranes have a similar tensile strength for the same polymer backbone (Table 2), indicating that the mechanical property of membranes depends on their polymer backbone, rather than the side chains.[36]. To study the chemical stability of the AEMs, the ampules were immersed in a 1.5 M VO^{2+}/3 M H_2SO_4 electrolyte solution for 30 days at 25 °C. An 11.37 and 10.96 wt % weight loss can be observed for ImPPO and BImPPO membranes, respectively, which indicate the good chemical stability of the PPO-based AEMs. The photographs show that ImPPO and BImPPO membranes remained intact after the chemical stability test (insets, Figure 3), which also proved that the polymer backbone we selected was suitable for VRFB application.

Table 2. Mechanical Properties of Nafion, ImPPO, and BImPPO Membrane

samples	tensile modulus (MPa)	tensile strength (MPa)	elongation at break (%)
Nafion212	320 ± 12	11 ± 1.0	85.0 ± 5.0
ImPPO	464 ± 15	22 ± 0.3	30.1 ± 0.5
BImPPO	496 ± 22	27 ± 0.6	29.9 ± 3.2

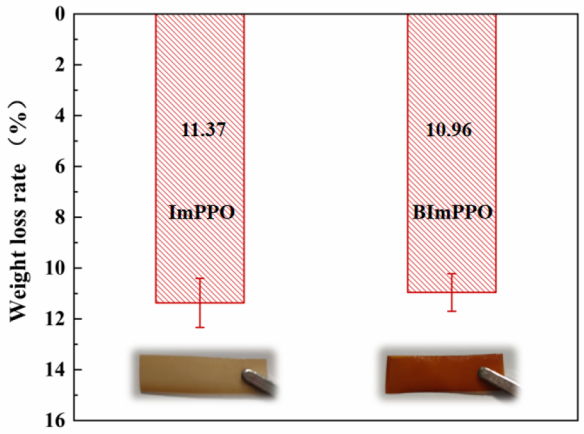

Figure 3. Weight loss and appearance (insets) of ImPPO and BImPPO membranes after immersing in 1.5 M VO^{2+}/3 M H_2SO_4 for 30 days.

3.4. Vanadium Permeability. High vanadium permeability, one of the most significant barriers to the application of IEMs in VRFBs, directly influences the performance of the assembled VRFB.[37,38] Figure 4a shows the changing curve of VO^{2+} concentration in the diffusion electrolytic cell assembled with ImPPO, BImPPO, and Nafion 212 membranes and the vanadium permeability of the corresponding membranes of 3.2 × 10^{-9}, 2.9 × 10^{-9}, and 8.8 × 10^{-9} cm^2 s^{-1}, respectively (Figure 4b). The values for ImPPO and BImPPO membranes are lower than that of the Nafion212 membrane, owing to the susceptibility of the imidazolium cations to the Donnan effect. The value for BImPPO is slightly lower than that of the ImPPO, probably because of the lower SR lead to a more compact structure of BImPPO. The low vanadium permeability of the membrane means there is less contamination from positive and negative VRFBs, which leads to an improved VRFB performance.

3.5. VRFB Single Cell Performance. ImPPO, BImPPO, and Nafion212 were used to assemble VRFBs, and the efficiency of VRFBs was evaluated at 40−140 mA cm^{-2} (Figure 5). With an increase in current density, the charge time was shortened considerably, causing vanadium ion cross-contamination and self-discharge reduction, therefore improving the Coulombic efficiency (CE) of VRFBs. The CE of the VRFBs

https://doi.org/10.1021/acsomega.3c01846
ACS Omega 2023, 8, 16506−16512

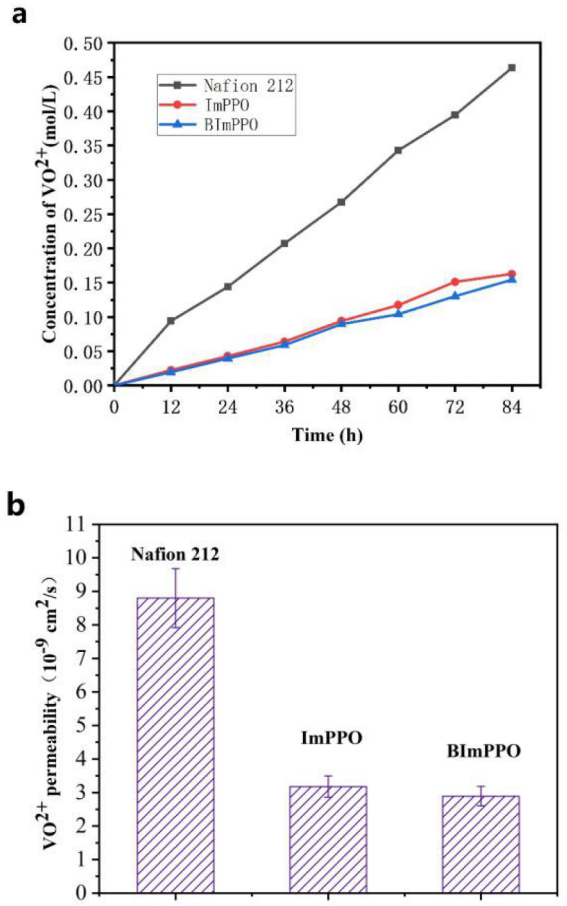

Figure 4. Changing curve of VO^{2+} concentration in the diffusion cells with time (a) and the vanadium permeability of membranes (b).

with ImPPO and BImPPO membranes (98.5% and 99.8%, respectively) was higher than that of the Nafion212 (92.4%), which is consistent with the vanadium permeability of the membranes. This is because the low vanadium permeability results in lower positive and negative cross-contamination, which reduces the self-discharge and increases the CE of the VRFBs. Moreover, the VE and EE of the single cells assembled with the ImPPO and BImPPO membranes were 82.2% and 79.5% and 86.7% and 84.5%, respectively. All of these values were significantly higher than those for the VRFB assembled with a Nafion 212 membrane (79.2% and 70.6%, respectively) because of the lower AR of the ImPPO and BImPPO membranes. These results indicate that ImPPO and BImPPO membranes have high potential for application to VRFBs. Furthermore, the VRFB assembled with BImPPO demonstrated better performance than that assembled with the ImPPO membrane owing to its higher conductivity.

The long-term stability of the VRFB is an indication of the performance of the membranes. The discharge capacities of all the VRFBs decayed gradually with increasing cycle number. The discharge capacity retentions for the VRFBs with ImPPO and BImPPO were 30.7% and 45.5%, respectively, after 200 cycles, which is much higher than that of Nafion 212 (14.7%, Figure 6a). This is because of the low vanadium permeability of ImPPO and BImPPO membranes compared to Nafion 212 owing to the effects of Donnan exclusion on the imidazolium cations. Figure 6b shows the cycling performances of the ImPPO, BImPPO, and Nafion 212 membrane. The VRFBs with ImPPO and BImPPO exhibited EE values of 82.9% and 76.2%, respectively, even after 200 cycles, which are much higher than that of 68.1% in a VRFB with Nafion 212. The low-capacity decay is beneficial for the long-term operation of VRFBs and indicates the excellent stability of the ImPPO and BImPPO membranes. The VRFB with the BImPPO membrane showed the best stable charge−discharge platform and highest charge−discharge capacity owing to its high conductivity and low vanadium permeability resulting from the long-pendant alkyl-side-chain and was the overall highest-performing VRFB.

4. CONCLUSIONS

In summary, imidazolium-functionalized PPO with and without long-pendant alkyl-side-chains was synthesized and characterized. The BImPPO membrane with long-pendant alkyl-side-chain bis-imidazolium cations exhibited higher conductivity than the ImPPO without long-pendant alkyl side chains. Although the BImPPO and ImPPO membranes possess similar IECs, the BImPPO exhibits higher conductivity than the ImPPO for the hydrophilic/hydrophobic phase separation formed in the BImPPO membrane. Both the BImPPO and ImPPO membranes demonstrated lower vanadium permeability than that of Nafion 212 for the Donnan effect of imidazolium cations. Meanwhile, the VRFBs assembled with ImPPO and BImPPO membranes had CEs of 98.5% and 99.8%, respectively, at 140 mA cm^{-2}, while the one assembled with Nafion212 showed a value of 95.8% under the same conditions. Furthermore, compared with that of ImPPO and Nafion 212 membranes, the VRFB assembled with the BImPPO membrane showed a much better capacity retention This study demonstrates that BImPPO membranes are suitable for application in VRFBs.

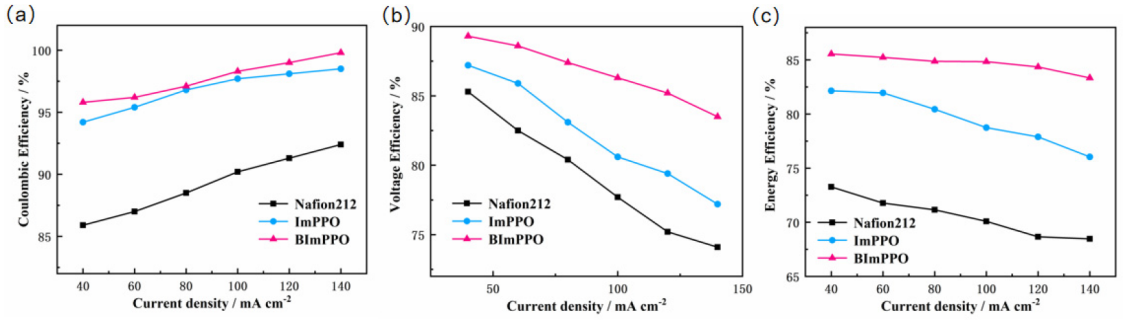

Figure 5. CE (a), VE (b), and EE (c) of VRFBs assembled with Nafion212, ImPPO, and BImPPO membranes.

https://doi.org/10.1021/acsomega.3c01846
ACS Omega 2023, 8, 16506−16512

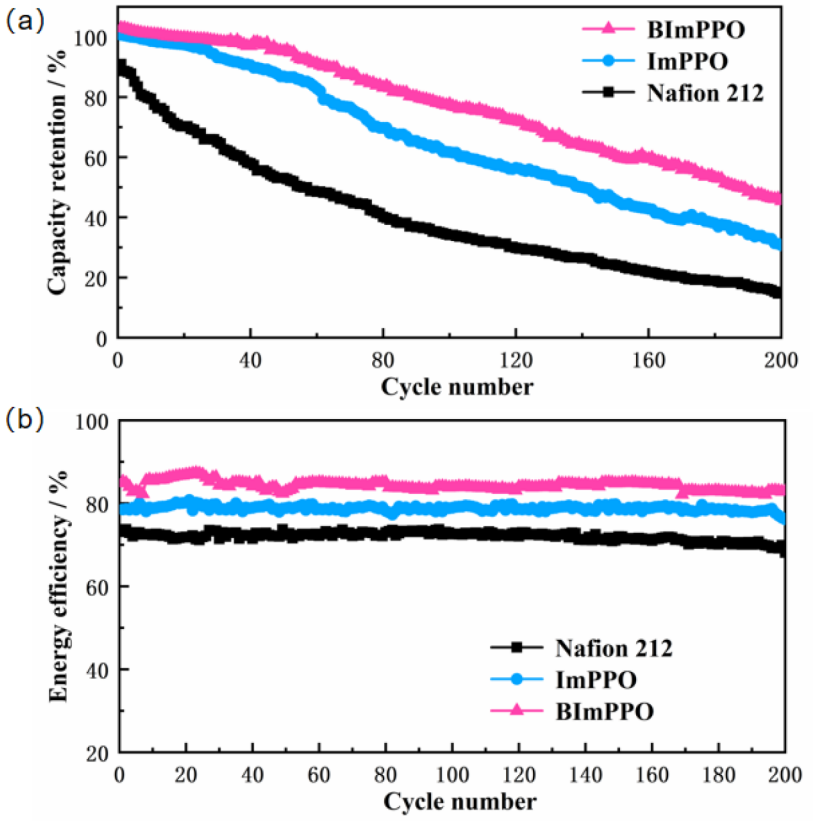

Figure 6. Discharge capacity decay (a) and long-term stability test (b) of VRFBs assembled with ImPPO, BImPPO, and Nafion212 membranes at 80 mA cm^{-2}.

■ ASSOCIATED CONTENT

Supporting Information

The Supporting Information is available free of charge at https://pubs.acs.org/doi/10.1021/acsomega.3c01846.

^{1}H NMR spectra of BrPPO and 2,3-dimethyl-1-(6-(2-methylimidazol-1-yl) hexyl)-imidazolium iodide (PDF)

■ AUTHOR INFORMATION

Corresponding Author

Bencai Lin − *School of Materials Science and Engineering, Jiangsu Collaborative Innovation Center of Photovolatic Science and Engineering, Changzhou University, Changzhou, Jiangsu 213164, China;* orcid.org/0000-0002-0826-8090; Email: linbencai@cczu.edu.cn

Authors

Jing Li − *School of Materials Science and Engineering, Jiangsu Collaborative Innovation Center of Photovolatic Science and Engineering, Changzhou University, Changzhou, Jiangsu 213164, China*

Fei Xu − *School of Materials Science and Engineering, Jiangsu Collaborative Innovation Center of Photovolatic Science and Engineering, Changzhou University, Changzhou, Jiangsu 213164, China*

Weishu Chen − *School of Materials Science and Engineering, Jiangsu Collaborative Innovation Center of Photovolatic Science and Engineering, Changzhou University, Changzhou, Jiangsu 213164, China*

Yuyang Han − *School of Materials Science and Engineering, Jiangsu Collaborative Innovation Center of Photovolatic Science and Engineering, Changzhou University, Changzhou, Jiangsu 213164, China*

Complete contact information is available at: https://pubs.acs.org/10.1021/acsomega.3c01846

Notes

The authors declare no competing financial interest.

■ ACKNOWLEDGMENTS

This work was supported by the National Natural Science Foundation of China (No. 51973022), Postgraduate Research and Practice Innovation Program of Jiangsu Province (KYCX223004), and Qing Lan project of Jiangsu province.

■ REFERENCES

(1) Vudata, S. P.; Bhattacharyya, D. Transient Modeling of a Vanadium Redox Flow Battery and Real- Time Monitoring of Its Capacity and State of Charge. *Ind. Eng. Chem. Res.* **2022**, *61* (48), 17557−17571.

(2) Park, D. J.; Jeon, K. S.; Ryu, C. H.; Hwang, G. J. Performance of the all-vanadium redox flow battery stack. *J. Ind. Eng. Chem.* **2017**, *45*, 387−390.

(3) Helms, B. A.; Seferos, D. S. Virtual Issue: Designing Polymers for Use in Electrochemical Energy Storage Devices. *Macromolecules* **2019**, *52* (4), 1349−1353.

(4) Xiong, P.; Zhang, L. Y.; Chen, Y. Y.; Peng, S. S.; Yu, G. H. A Chemistry and Microstructure Perspective on Ion-Conducting Membranes for Redox Flow Batteries. *Angew. Chem.-Int. Ed.* **2021**, *60* (47), 24770−24798.

(5) Shi, Y.; Eze, C.; Xiong, B. Y.; He, W. D.; Zhang, H.; Lim, T. M.; Ukil, A.; Zhao, J. Y. Recent development of membrane for vanadium

redox flow battery applications: A review. *Appl. Energy* **2019**, *238*, 202−224.
(6) Jiang, B.; Wu, L. T.; Yu, L. H.; Qiu, X. P.; Xi, J. Y. A comparative study of Nafion series membranes for vanadium redox flow batteries. *J. Membr. Sci.* **2016**, *510*, 18−26.
(7) Grosse Austing, J.; Nunes Kirchner, C.; Komsiyska, L.; Wittstock, G. Layer-by-layer modification of Nafion membranes for increased lifetime and efficiency of vanadium/air redox flow batteries. *J. Membr. Sci.* **2016**, *510*, 259−269.
(8) Lu, Y.; Lin, S.; Cao, H.; Xia, Y.; Xia, Y.; Xin, L.; Qu, K.; Zhang, D.; Yu, Y.; Huang, K.; Jing, W.; Xu, Z.; et al. Efficient proton-selective hybrid membrane embedded with polydopamine modified MOF-808 for vanadium flow battery. *J. Membr. Sci.* **2023**, *671*, 121347.
(9) Li, J. C.; Liu, J.; Xu, W. J.; Long, J.; Huang, W. H.; He, Z.; Liu, S. Q.; Zhang, Y. P. A Sulfonated Polyimide/Nafion Blend Membrane with High Proton Selectivity and Remarkable Stability for Vanadium Redox Flow Battery. *Membranes* **2021**, *11* (12), 946.
(10) Li, J.; Xu, F.; Chen, Y. B.; Han, Y. Y.; Lin, B. C. Sulfonated Poly(ether Ether Ketone)/Sulfonated Covalent Organic Framework Composite Membranes with Enhanced Performance for Application in Vanadium Redox Flow Batteries. *ACS Appl. Energy Mater.* **2022**, *5* (12), 15856−15863.
(11) Quan, Y. Z.; Wang, G.; Li, A. F.; Wei, X. Y.; Li, F.; Zhang, J.; Chen, J. W.; Wang, R. L. Novel sulfonated poly(ether ether ketone)/triphenylamine hybrid membrane for vanadium redox flow battery applications. *RSC Adv.* **2019**, *9* (7), 3838−3846.
(12) Li, G.; Wang, G.; Wei, S. G.; Yu, Y.; Li, X. S.; Zhang, J.; Chen, J. W.; Wang, R. L. Side-Chain Grafting-Modified Sulfonated Poly(ether ether ketone) with Significantly Improved Selectivity for a Vanadium Redox Flow Battery. *Ind. Eng. Chem. Res.* **2023**, *62*, 2460.
(13) Kim, K.; Heo, P.; Han, J.; Kim, J.; Lee, J. C. End-group cross-linked sulfonated poly(arylene ether sulfone) via thiol-ene click reaction for high-performance proton exchange membrane. *J. Power Sources* **2018**, *401*, 20−28.
(14) Thiam, B. G.; El Magri, A.; Vaudreuil, S. An overview on the progress and development of modified sulfonated polyether ether ketone membranes for vanadium redox flow battery applications. *High Perform. Polym.* **2022**, *34* (2), 131−148.
(15) Qian, J. F.; Cai, S. J.; Hu, J. X.; Wang, C. Y.; Li, G. Preparation and Properties of Quaternary Ammonium Anion Exchange Membranes with Flexible Side Chains for the Vanadium Redox Flow Battery. *Ind. Eng. Chem. Res.* **2023**, *62*, 2719.
(16) Che, X. F.; Tang, W. Q.; Dong, J. H.; Aili, D.; Yang, J. S. Anion exchange membranes based on long side-chain quaternary ammonium-functionalized poly(arylene piperidinium)s for vanadium redox flow batteries. *Sci. China-Mater.* **2022**, *65* (3), 683−694.
(17) Yan, X. M.; Zhang, C. M.; Dai, Y.; Zheng, W. J.; Ruan, X. H.; He, G. H. A novel imidazolium-based amphoteric membrane for high-performance vanadium redox flow battery. *J. Membr. Sci.* **2017**, *544*, 98−107.
(18) Wang, Z. Q.; Zhang, S. H.; Liu, Q.; Zhuo, L.; Liu, Z. Y.; Xu, P. Q.; Wang, D. H.; Weng, Z. H.; Jian, X. G. Pyridinium functionalized poly(phthalazinone ether ketone) with pendant phenyl groups porous membranes for vanadium flow battery application by vapor induced phase separation. *J. Membr. Sci.* **2022**, *656*, 120646.
(19) Lu, D.; Wen, L. L.; Nie, F.; Xue, L. X. Synthesis and investigation of imidazolium functionalized poly(arylene ether sulfone)s as anion exchange membranes for all-vanadium redox flow batteries. *RSC Adv.* **2016**, *6* (8), 6029−6037.
(20) Wang, W.; Xu, M.; Wang, S.; Xie, X.; Lv, Y.; Ramani, V. K. Bifunctional Crosslinking Agents Enhance Anion Exchange Membrane Efficacy for Vanadium Redox Flow Batteries. *ACS Appl. Mater. Interfaces* **2022**, *14* (44), 49446−49453.
(21) Chu, F. Q.; Chu, X. F.; Lv, T.; Chen, Z. Y.; Ren, Y. R.; Zhang, S.; Yuan, N. Y.; Lin, B. C.; Ding, J. N. Amphoteric Membranes Based on Sulfonated Polyether Ether Ketone and Imidazolium-Functionalized Polyphenylene Oxide for Vanadium Redox Flow Battery Applications. *ChemElectroChem.* **2019**, *6* (19), 5041−5050.
(22) Charyton, M.; Iojoiu, C.; Fischer, P.; Henrion, G.; Etienne, M.; Donten, M. L. Composite Anion-Exchange Membrane Fabricated by UV Cross-Linking Vinyl Imidazolium Poly(Phenylene Oxide) with Polyacrylamides and Their Testing for Use in Redox Flow Batteries. *Membranes* **2021**, *11* (6), 436.
(23) Chen, Y.; Li, Y. Y.; Xu, J. Q.; Chen, S. Y.; Chen, D. Y. Densely Quaternized Fluorinated Poly(fluorenyl ether)s with Excellent Conductivity and Stability for Vanadium Redox Flow Batteries. *ACS Appl. Mater. Interfaces* **2021**, *13* (16), 18923−18933.
(24) Barjola, A.; Reyes-Rodriguez, J. L.; Solorza-Feria, O.; Gimenez, E.; Compan, V. Novel SPEEK-ZIF-67 Proton Exchange Nanocomposite Membrane for PEMFC Application at Intermediate Temperatures. *Ind. Eng. Chem. Res.* **2021**, *60* (25), 9107−9118.
(25) He, Y. B.; Si, J. J.; Wu, L.; Chen, S. L.; Zhu, Y.; Pan, J. F.; Ge, X. L.; Yang, Z. J.; Xu, T. W. Dual-cation comb-shaped anion exchange membranes: Structure, morphology and properties. *J. Membr. Sci.* **2016**, *515*, 189−195.
(26) Zhu, L.; Pan, J.; Wang, Y.; Han, J. J.; Zhuang, L.; Hickner, M. A. Multication Side Chain Anion Exchange Membranes. *Macromolecules* **2016**, *49* (3), 815−824.
(27) Dang, H. S.; Jannasch, P. High-Performing Hydroxide Exchange Membranes with Flexible Tetra-Piperidinium Side Chains Linked by Alkyl Spacers. *ACS Appl. Energy Mater.* **2018**, *1* (5), 2222−2231.
(28) Li, J. M.; Liu, Q.; Tian, L.; Ma, W. L.; Wang, F. H.; Wang, Z. Q.; Zhu, H. Novel poly(carbazole-butanedione) anion exchange membranes constructed by obvious microphase separation for fuel cells. *Int. J. Hydrog. Energy* **2022**, *47* (75), 32262−32272.
(29) Marinkas, A.; Struzynska-Piron, I.; Lee, Y.; Lim, A.; Park, H. S.; Jang, J. H.; Kim, H. J.; Kim, J.; Maljusch, A.; Conradi, O.; et al. Anion-conductive membranes based on 2-mesityl-benzimidazolium functionalised poly(2,6-dimethyl-1,4-phenylene oxide) and their use in alkaline water electrolysis. *Polymer* **2018**, *145*, 242−251.
(30) Han, J. J.; Peng, Y. Q.; Lin, B. C.; Zhu, Y. C.; Ren, Z. D.; Xiao, L.; Zhuang, L. Hydrophobic Side-Chain Attached Polyarylether-Based Anion Exchange Membranes with Enhanced Alkaline Stability. *ACS Appl. Energy Mater.* **2019**, *2* (11), 8052−8059.
(31) Lin, B. C.; Xu, F.; Chu, F. Q.; Ren, Y. R.; Ding, J. N.; Yan, F. Bis-imidazolium based poly(phenylene oxide) anion exchange membranes for fuel cells: the effect of cross-linking. *J. Mater. Chem. A* **2019**, *7* (21), 13275−13283.
(32) Liu, L.; Li, D. F.; Xing, Y.; Li, N. W. Mid-block quaternized polystyrene-b-polybutadiene-b-polystyrene triblock copolymers as anion exchange membranes. *J. Membr. Sci.* **2018**, *564*, 428−435.
(33) Lee, K. H.; Chu, J. Y.; Mohanraj, V.; Kim, A. R.; Song, M. H.; Yoo, D. J. Enhanced ion conductivity of sulfonated poly(arylene ether sulfone) block copolymers linked by aliphatic chains constructing wide-range ion cluster for proton conducting electrolytes. *Int. J. Hydrog. Energy* **2020**, *45* (53), 29297−29307.
(34) Duan, X. L.; Wang, C. W.; Wang, T. L.; Xie, X. L.; Zhou, X. P.; Ye, Y. S. Comb-shaped anion exchange membrane to enhance phosphoric acid purification by electro-electrodialysis. *J. Membr. Sci.* **2019**, *573*, 64−72.
(35) Tang, W. Q.; Mu, T.; Che, X. F.; Dong, J. H.; Yang, J. S. Highly Selective Anion Exchange Membrane Based on Quaternized Poly-(triphenyl piperidine) for the Vanadium Redox Flow Battery. *ACS Sustain. Chem. Eng.* **2021**, *9* (42), 14297−14306.
(36) Jin, Y. P.; Wang, T.; Che, X. F.; Dong, J. H.; Li, Q. F.; Yang, J. S. Poly(arylene pyridine)s: New alternative materials for high temperature polymer electrolyte fuel cells. *J.Power Sources.* **2022**, *526*, 231131.
(37) Dai, W. J.; Shen, Y.; Li, Z. H.; Yu, L. H.; Xi, J. Y.; Qiu, X. P. SPEEK/Graphene oxide nanocomposite membranes with superior cyclability for highly efficient vanadium redox flow battery. *J. Mater. Chem. A* **2014**, *2* (31), 12423−12432.
(38) Thiam, B. G.; Vaudreuil, S. Review-Recent Membranes for Vanadium Redox Flow Batteries. *J. Electrochem. Soc.* **2021**, *168* (7), 070553.

https://doi.org/10.1021/acsomega.3c01846
ACS Omega 2023, 8, 16506−16512